Proceedings of the ASME 2013 32nd International Conference on Ocean, Offshore and Arctic Engineering
OMAE2013
June 9-14, 2013, Nantes, France

OMAE2013-10445

WET VIBRATION OF AXIALLY LOADED ELASTICALLY SUPPORTED PLATES TO MOVING LOADS: AIRCRAFT LANDING ON FLOATING AIRPORTS

N.Datta and J.D.Thekinen
Department of Ocean Engineering and Naval Architecture, Indian Institute of Technology, Kharagpur, INDIA.
Corresponding author : ndatta@naval.iitkgp.ernet.in

ABSTRACT

Dynamic analysis of thin rectangular elastically supported stiffened plates with axial loads is presented. A floating airport is modeled as a horizontal Kirchhoff's plate, which is elastically supported at the ends; and is subjected to the impact of aircrafts landing and deceleration over its length. This sets the free-free-free-free plate into high-frequency vibration, causing flexural stress waves to travel over the plate. First, the beam natural frequencies and modeshapes in either direction are generated with these complexities. The Eigen value analysis of the governing differential equation is done, using the weighted summation of the product of the beam modes. The accuracy of the frequencies is compared with those from FEA studies. The radiation pressure on the bottom side of the plate is included to reduce the frequencies by the added-mass effect. The plate is then subjected to decelerating shock loads. The vibratory response is analyzed by the computationally efficient normal mode analysis. The amplification factor vs. the taxiing time of the moving load is generated.
Keywords Plate vibration, Shock loads, Normal mode analysis, Added mass.

1. Introduction

The increase in the world population has been congesting the inhabitable areas, leading to land being at a premium. Smaller and island countries (e.g. Japan) have been foraying into floating cities and airports, in an attempt to "reclaim" artificial "land" area on the sea. Design of such VLFS (Very Large Floating Structure) has been gaining relevance over the past few decades. Floating airports are subject to impact loads with aircrafts land over them, followed by a transient load of the taxiing of the craft. This causes dynamic deflections and stresses in the VLFS, which must be analyzed to ensure a sound structural design of the highly expensive fabrication. If the sea is calm (sea state < 3), the fluid added to the radiation pressure which reduced the natural frequency of the plate, thereby making it tender. Higher sea states cause waves to act as irregular force on the structure, leading to global bending moments and shear stresses, in addition to the transient impact load of the aircraft.

Young (1950) analyzed the free vibration of plates by the *Ritz method*, with various boundary conditions. Saha et al (2004) studied the higher-order large-amplitude vibrations of plates for different boundary conditions. Wang et al (2005) perfected the modeshape functions of plates with different boundary conditions. Yeh et al (2006) delved into the numerical aspects of free vibration analysis of plates. Yu et al (2008) studied the numerical convergence of the frequencies of square plates with various boundary conditions. Chen et al (2009) generated the modeshapes of rectangular plates experimentally, comparing them with FEA.

Meyerhoff (1970) calculated the added masses of rectangular plates, by calculating the dipole strength densities corresponding to each plate modeshape. Joseph et al (1990) studied the wet vibration of square plates of different material and fluid densities. Kwak (1996) calculated the wet vibration frequencies of thin rectangular CCCC and SSSS plates by modal analysis, considering two different boundary value problems. Cheung and Zhou (2000) extended this study by considering different volumes of fluid in contact with the plate. The above work, however, is limited to free vibration only.

Robinson and Palmer (1990) theoretically formulated the frequency parameter of a FFFF plate in contact with water on one side, stopping short of calculating the frequencies and modeshapes. Kagemoto et al (1998) calculated the wave-response of a VLFS using substructure models using FEA, and experimentally. This work did not take any shock loads into account. It studied only one case of plate size and configuration, but could not generalize the frequencies, modeshapes, added masses, and dynamic loading factors. Endo (2000) used FEA to study the VLFS response due to aircraft landing/takeoff. Seto et al (2005) studied the two-

way coupled Mega-Float vibratory response due to wave action. Hashemi et al (2010) studied the free vibration of elastically supported plates with water on one side, using the Ritz method.

None of the above literature studied the impact-induced vibration of elastically supported plates, in contact with water on one side, due to aircraft landing, using the modal analysis, bypassing the computationally expensive and commercial codes.

In this paper, a floating airport is modeled as a rectangular plate with water on one side, supported on the edges by elastic supports. Moorings cause axial tension in the plate, which makes the structure stiffer (increased natural frequencies. The sea is assumed to be calm, i.e. the plate vibration occurs in calm water. A MATLAB code has been written for the dry and wet dynamic analysis. First, the free (dry) vibration analysis of the plate is done using the Galerkin's method. The natural frequencies and modeshapes of the plate are generated for different aspect ratios. The structure is assumed to be very lightly damped. The radiation pressure has been included with the source distribution technique, leading to added masses associated with each modeshape and the corresponding reduced (wet) natural frequencies. The radiation damping is negligible, given the high frequencies of the vibrations.

This is followed by a forced vibration analysis of the plate, due to the impact of the landing aircraft, which decelerates to zero velocity. The transient force sets the plate in vibrations, exciting all its natural frequencies to various extents. The dynamic analysis with the normal mode summation method; and the corresponding static analysis is done by Galerkin's method. The global maximum dynamic deflection is normalized by the global maximum static deflection to generate the Dynamic Loading Factor (DLF) for various taxiing time and decelerations. The modal participation of the plate modeshapes in the total deflection is also studied to establish the modal truncation guidelines. Impact and transient loads cause the participation of the higher order modes. Optimized taxiing duration and decelerations has been recommended, which leads to the minimum dynamic deflections and stresses.

2. Problem formulation

The floating airport is modeled as a solid Kirchhoff's plate (Fig.1), of length L, width B, thickness h, flexural rigidity D, floating in contact with water of density ρ_{water}, and supported over its edges by elastic supports of spring constant K. The water depth is considered to be 'shallow' since the dimensions of the VLFS are in the order of kilometers, while the water depth near the shore (continental shelf) is in the order of metres. The plate is tethered by mooring lines, which cause an axial tension of N_x along the X-direction, and N_y the Y-direction. The structure is considered to be lightly damped, with the damping ratio < 5%. Damping reduces the first dynamic deflection overshoot of the structure (over the static deflection), thereby reducing the dynamic loading factor. Proportional damping has been used here. The radiation damping is assumed to be zero. The high-frequency limit of the vibration causes the air-water interface to behave like a rigid-lid, having no outgoing waves. The radiation pressure is almost nearly in phase with the acceleration of the body ('added mass' effect).

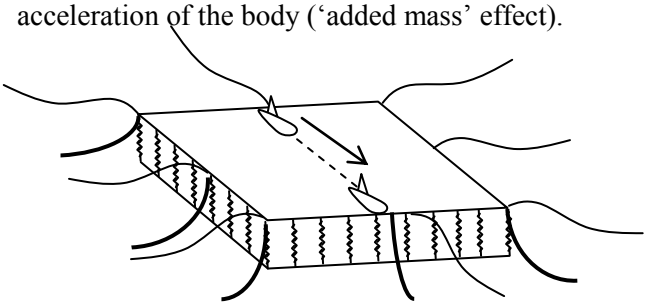

Fig. 1 Elastically supported plate.

The aircraft-landing dynamic force is modeled as a Heaviside step function (w.r.t time), which initially (at position A) has a velocity 'u' m/sec along the length of the plate, and decelerated to zero velocity (at position B), over a taxiing distance 'S' m, and for a taxiing duration of t_{tax}. The deceleration is 'a' m/s^2. The impact F and the transient force F(x,t) set the plate into small-amplitude high-frequency vibrations. The initial velocity of the aircraft at landing (position A), i.e. 'u' m/sec, is considered to be a constant. The final velocity, at position B, is zero. The deceleration $a = \frac{u^2}{2S}$ and the taxiing distance $S = ut_{tax} - \frac{1}{2}at_{tax}^2$. Deceleration 'a' va. t_{tax} vary as a rectangular hyperbola. A dual parametric variation may been used in this study : (a) the taxiing distance 'S' is kept constant, varying the deceleration 'a', and thus the taxing time t_{tax}, and (b) the deceleration 'a' is kept constant, varying the taxiing distance 'S' and thus the taxiing time t_{tax}.

3. Analysis methodology

The cross-section view of the floating airport, at y = B/2, is shown in Fig.2. The aircraft lands at position A, with an initial horizontal velocity 'u' m/sec, and decelerates to rest at position B. The vertical velocity of the craft is assumed to be nearly zero, and there is no vertical impact on the plate due to the landing. The moving load sets the airport into flexural vibrations, exciting all the natural frequencies and plate modeshapes to various extents, causing tensile and shear stress wave patterns to travels across the plate.

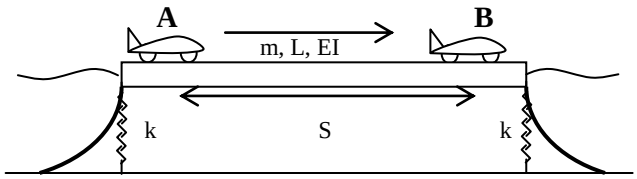

Fig. 2 Elastically supported beam.

3.1 Free Vibration : elastically supported beam

The GDE of free vibration of an elastically supported beam, under axial tension, is given as :

$m\frac{\partial^2 z(x,t)}{\partial t^2} + EI\frac{\partial^4 z(x,t)}{\partial x^4} - N_x\frac{\partial^2 z(x,t)}{\partial x^2} = 0$, subject to:

$z''(0) = z''(L) = 0, EIz'''(0) = -Kz(0),\ EIz'''(L) = -Kz(L),$

i.e. the end bending moment is zero, while the shear force at the ends balances the spring force due to the end deflection. As K→0, the plate behaves like a Free-Free (FF) beam, while as K→∞, the beam behaves as a simply supported (SS) beam. Each support generates a shear force at the ends, except for the Free-Free beam. The end shear force for a simply-supported beam is $EI\left(\frac{j\pi}{L}\right)^3$ for the j[th] modeshape. For K< ∞, the end shear force is a % of $EI\left(\frac{j\pi}{L}\right)^3$, and thus, it is denoted as a % support. For K = 0, the end shear force vanishes, and we get a 0% supported beam or a free-free beam. The dynamic deflection is expressed as $z(x,t) = G(x)F(t)$. Using the method of separation of variables, $G^{IV}(x) = \frac{m\omega^2}{EI}G(x)$ or $G^{IV}(x) = \beta^4 G(x)$. The general solution of the 4[th] order ODE is :

$$G(x) = G_1\cos\beta x + G_2\sin\beta x + G_3\cosh\beta x + G_4\sinh\beta x.$$

The constants G1, G2, G3, G4 are calculated from the boundary conditions:

$$-G_1 + G_3 = 0;$$

$$-G_1\cos\beta L - G_2\sin\beta L + G_3\cosh\beta L + G_4\sinh\beta L = 0;$$

$$\frac{k}{EI}G_1 + \beta^3 G_2 + \frac{k}{EI}G_3 - \beta^3 G_4 = 0;$$

$$\left\{\frac{k}{EI}\cos\beta L - \beta^3\sin\beta L\right\}G_1 + \left\{\frac{k}{EI}\sin\beta L + \beta^3\cos\beta L\right\}G_2$$

$$+\left\{\frac{k}{EI}\cosh\beta L - \beta^3\sinh\beta L\right\}G_3$$

$$+\left\{\frac{k}{EI}\sinh\beta L - \beta^3\cosh\beta L\right\}G_4 = 0.$$

Writing the above system of equations in the matrix form, and equating the determinant to zero (for a non-trivial solution) generates the frequency equation, which is a transcendental equation, satisfied by an infinite number of unique values β, each corresponding to a unique natural frequency. The Eigen vectors of the above system generate the constants G1, G2, G3, G4; and thus the modeshapes.

3.2 Free Dry Vibration : elastically supported plate

The GDE of free vibration of an elastically supported Kirchhoff's plate is expressed as follows :

$$m\frac{\partial^2 z(x,y,t)}{\partial t^2} + D\left[\frac{\partial^4 z(x,y,t)}{\partial x^4} + 2\frac{\partial^4 z(x,y,t)}{\partial x^2\partial y^2} + \frac{\partial^4 z(x,y,t)}{\partial y^4}\right]$$

$$-N_x\frac{\partial^2 z(x,y,t)}{\partial x^2} - N_y\frac{\partial^2 z(x,y,t)}{\partial y^2} - N_{xy}\frac{\partial^2 z(x,y,t)}{\partial x\partial y} = 0$$

The bending moment M_x and M_y are zero at the ends, and the shear force at the edges equals the spring force produced due to the deflection of the modeshape. As K→0, the plate behaves like a Free-Free-Free-Free (FFFF) plate, while as K→∞, the plate behaves as a simply supported (SSSS) plate. Axial tension increases the natural frequencies of the structure, without influencing the modeshapes. The total out-of-plane dynamic deflection z(x,y,t) is a function of space and time. Separating the variables into space and time, we assume $\Phi_k(x,y)$ as the k[th] spatial shape function, and $q_k(t)$ as the temporal function of the k[th] vibratory mode. The dynamic deflection of the plate is approximately

$z(x,y,t) = \sum_{k=1}^{\infty}\Phi_k(x,y)\,q_k(t)$ with the 3-D plate modeshape is defined as a series sum as follows :

$$\Phi_k(x,y) = \sum_{j=1}^{modex}\sum_{l=1}^{modey} A_{jl}^k\phi_j(x)\phi_l(y) = \sum_{j=1}^{modex}\sum_{l=1}^{modey} A_{jl}^k G_{jl}$$

i.e. $G_{jl}(x,y) = \phi_j(x)\phi_l(y)$, *modex* is the number of modes considered in the *x*-direction, *modey* is the

number of modes considered in the *y*-direction, and $\phi_j(x)$ and $\phi_l(y)$, are the respective 2-D beam modeshapes (orthogonal set of functions). A_{jl}^k is the amplitude of each $G_{jl}(x,y)$ for the kth natural frequency of vibration. The natural frequency is nondimensionalized by the factor $\sqrt{\frac{D}{mL^2B^2}}$.

3.3 Free Wet Vibration : elastically supported plate

The 3D boundary value problem of wet vibration of plates, with water on one side, is framed as shown in Fig.3. The flexible plate has a semi-infinite fluid domain on one side, the other side being dry. Sides DA and BC are a part of the "rigid lid", formed by the high frequency limit of the combined free surface boundary condition. AB represents the flexible plate. Assuming inviscid, incompressible, irrotational flow, the velocity potential satisfies the Laplace equation in the fluid domain, subject to the following boundary conditions: (a) the normal velocity on DA and BC are zero, (b) the normal velocity on AB equals the structural velocity, (c) fluid velocity tends to zero at the far-field. Here, we define ψ*(x,y,z) as the velocity potential per unit structural velocity. The governing differential equation for the unforced, wet, damped vibration of a Kirchhoff's plate is

$$\sum_{k=1}^{\infty} m\Phi_k(x,y)\frac{d^2q_k(t)}{dt^2}+\sum_{k=1}^{\infty} D\nabla^4\Phi_k(x,y)q_k(t)=$$

$$-\rho_{water}\sum_{k=1}^{\infty}\Psi_k^*(x,y,0)\frac{d^2q_k(t)}{dt^2}\ .$$

$$\Rightarrow\ \sum_{k=1}^{\infty}\left[m+\rho_{water}\left\{\int_{\varepsilon}2\Phi_k(\xi,\eta)\ G_{PQ}dS_Q\right\}\right]\Phi_k\ \ddot{q}_k(t)+$$

$$\sum_{k=1}^{\infty} D\nabla^4\Phi_k(x,y)\,q_k(t)=0;$$

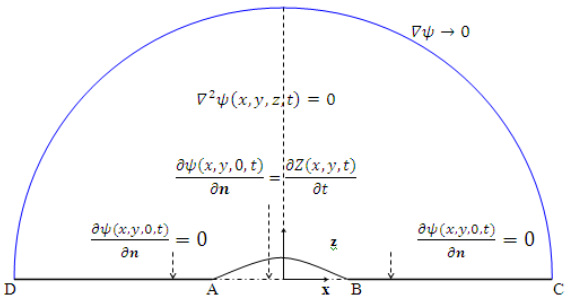

Fig.3 Boundary Value Problem

Pre-multiplying by the rth plate modeshape $\Phi_r(x,y)$ and integrating over the surface area of the plate gives the generalized mass, generalized added mass, and generalized stiffness.

$$\sum_{k=1}^{\infty}\left[\iint_{LB}\Phi_r(x,y)m\Phi_k(x,y)dxdy\right]\frac{d^2q_k(t)}{dt^2}$$

$$+\rho_{water}\sum_{k=1}^{\infty}\left[\iint_{LB}\Phi_r(x,y)\Psi_k^*(x,y,0)dxdy\right]\frac{d^2q_k(t)}{dt^2}$$

$$+\sum_{k=1}^{\infty}\left[\iint_{LB}\Phi_r(x,y)D\nabla^4\Phi_k(x,y)dxdy\right]q_k(t)=0.$$

Or $\sum_{n=1}^{k}(M_{kn}\ddot{+}A_{kn})\,q_n(t)+\sum_{n=1}^{k}K_{kn}q_n(t)=0$; with the gen. added mass is $A_{kn}=\iint_{LB}\Phi(x,y)\rho_{water}\Psi(x,y,0)dxdy.$

The **N**on-dimensional **A**dded **V**irtual **M**ass **I**ncrement (NAVMI) factor depends only on the plate modeshape, and is independent of the present of tension in the plate. The outer surface of the plate (of is in contact with the fluid, and hence the fluid inertia is independent of the presence the marine craft) of frames/stiffeners on the inner surface of the plate. It is given as $NAVMI=\dfrac{\iint_{LB}\Phi_k(x,y)\Psi_k^*(x,y)dxdy}{\iint_{LB}\Phi_k(x,y)\Phi_k(x,y)dxdy}$.

3.4 Forced Vibration

The governing differential equation for forced vibration of an elastically supported, axially loaded plate under a moving point load is given as :

$$m\frac{\partial^2 z}{\partial t^2}+D\left[\frac{\partial^4 z}{\partial x^4}+2\frac{\partial^4 z}{\partial x^2\partial y^2}+\frac{\partial^4 z}{\partial y^4}\right]-N_x\frac{\partial^2 z}{\partial x^2}-N_y\frac{\partial^2 z}{\partial y^2}$$

$$-N_{xy}\frac{\partial^2 z}{\partial x\partial y}=F\delta(x-ut+\frac{1}{2}at^2).$$

This is solved by the computationally efficient normal mode summation method. Substitution of the modal superposition above, and integration with weighting functions over the space, gives the normal mode expansion of the governing differential equations as a function of time only, as :

$$\sum_{n=1}^{\infty}M_{km}\ddot{q}_n(t)\ +\sum_{n=1}^{\infty}K_{km}q_n(t)\ \sum_{n=1}^{\infty}N_{km}q_n(t)=gf_k(t),$$

or $[M]\{\ddot{q}(t)\}+[D]\{q(t)\}+[N]\{q(t)\}=\{gf(t)\}$.

Generalized mass $\equiv M_{kn} = \int_0^L \int_0^B \Phi_k(x,y)\Phi_n(x,y)dxdy$,

Gen. stiffness $\equiv K_{kn} = \int_0^L \int_0^B \Phi_k(x,y)\nabla^4\Phi_n(x,y)dxdy$,

Gen. axial load $\equiv N_{kn} = \int_0^L \int_0^B \Phi_k(x,y)\Phi_n''(x,y)dxdy$

Generalized forcing $\equiv gf_k = \int_0^L \int_0^B \Phi_k(x,y)F(x,y,t)dxdy$,

This is solved numerically by the stable Euler's implicit-explicit scheme, to calculate the principal coordinates $q_k(t)$ as a function of time. The principal coordinates are then multiplied by the corresponding plate modeshapes $\Phi_k(x,y)$ to generate the dynamic deflection z(x,y,t) as a function of space and time.

3.5 Static Deflection and DLF

The static deflection of the plate, at each time step, under the same loading configuration, is calculated as a function of space and time. The ratio of the dynamic deflection to the corresponding static deflection, under the equivalent loading conditions, is defined as the Dynamic Load Factor (DLF), i.e. $DLF = Max\left[\frac{Z(x,y,t)}{Max\ Z_{st}(x,y,t)}\right]$. The static deflection is calculated by solving the following equation using Galerkin's method which includes the contribution of all the 3-D plate modeshapes.

The classic static plate bending equation is : $D\nabla^4 Z(x,y,t) = F(x,y,t)$ which gives $Z_{st}(x,y,t) = \sum_{j=1}^{modex} \sum_{l=1}^{modey} H_{jl} G_{jl}(x,y)$. H_{jl} is the amplitude of the Galerkin's pre-multiplier $G_{jl}(x,y)$; and thus, it is the static counterpart of A_{jl}^k. Thus the DLF forms a very important design parameter for the structural designer, who does the static analysis of the corresponding area load only.

4. Results.

First, the free vibration results have been established to obtain the plate modeshapes, which are input in the mode-summation method of forced vibration analysis. The beam modeshapes are established for various end supports, which are used as admissible functions to generate the plate modeshapes.

4.1 Free Vibration : elastically supported beam

Table 1 shows the first five frequency parameters of elastically supported beams, for a range of factors $\frac{kL^3}{EI}$. For a support factor < 10^{-3}, the β values approach the frequency parameters of a FF beam, i.e. 4.73, 7.85, 10.99, etc. For a support factor > 10^6, the β values approach the frequency parameters of a SS beam, i.e. nπ. As seen in Fig.4, the sharpest change in the *fundamental* frequency parameter occurs for $10 < \frac{kL^3}{EI} < 100$. This change indicates the transition zone between the free-free beam behavior and the simply-supported beam behavior. However, for higher order modes, this sharp change occurs at the larger spring support factor (Fig.5). For the 10^{th} modeshape, the change occurs for $1000 < \frac{kL^3}{EI} < 100000$. As the wave number increases, the end slopes increase, leading to lower shear forces at the ends, and hence, larger range of free-free beam behavior.

The general expression of the modeshape for an elastically supported beam is given as

$G(x) = G_1\cos\beta x + G_2\sin\beta x + G_3\cosh\beta x + G_4\sinh\beta x.$

Putting in the boundary conditions produces a 4-equation system of the constant G1, G2, G3, G4. The correct Eigen vector (among four) must be chosen to generate the correct modeshapes, which are listed below in Table 2. The fundamental modeshape of elastically supported beams, for different support factors, are shown in Fig.6 below.

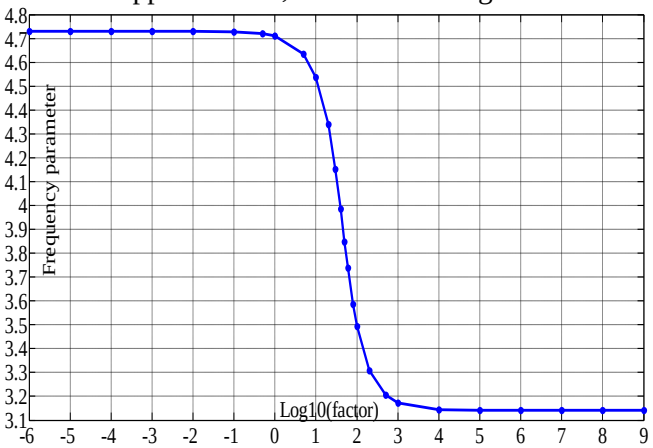

Fig.4 Fundamental βL vs. $\log_{10}$(factor)

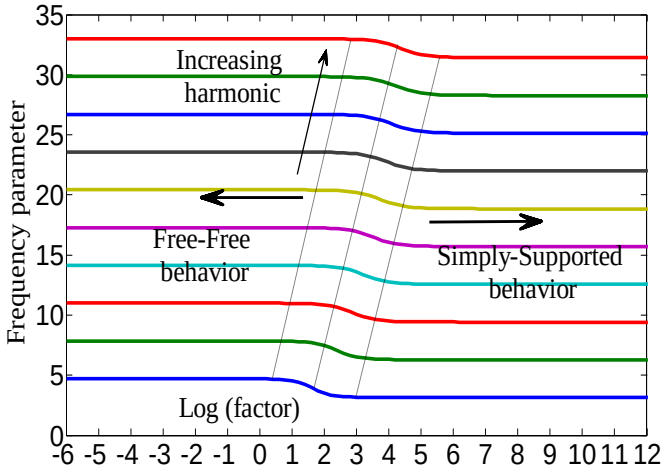

Fig.5 First 10 frequency parameters βL vs. $\log_{10}$(factor)

Table 1 Frequency parameters of the first 5 modes of elastically supported Euler-Bernoulli beams

Factor	βL_1	βL_2	βL_3	βL_4	βL_5
0.0000001	4.7300	7.8532	10.9956	14.1372	17.2788
0.000001	4.7300	7.8532	10.9956	14.1372	17.2788
0.00001	4.7300	7.8532	10.9956	14.1372	17.2788
0.0001	4.7300	7.8532	10.9956	14.1372	17.2788
0.001	4.7300	7.8532	10.9956	14.1372	17.2788
0.01	4.7282	7.8528	10.9955	14.1371	17.2787
0.1	4.7282	7.8528	10.9955	14.1371	17.2787
1	4.7111	7.8491	10.9941	14.1365	17.2784
10	4.5368	7.8121	10.9806	14.1301	17.2749
100	3.4929	7.4712	10.8507	14.0678	17.2405
1000	3.1731	6.5259	10.0776	13.5813	16.9408
10000	3.1447	6.3080	9.5071	12.7538	16.0471
100000	3.1419	6.2857	9.4331	12.5861	15.7463
1000000	3.1416	6.2834	9.4256	12.5684	15.7118
10000000	3.1416	6.2832	9.4249	12.5666	15.7084

Table 2 Eigen vectors of the frequency Equation matrix.

Support	**1000000**	**G1**	**G2**	**G3**	**G4**
	Mode 1	0	1	0	0
	Mode 2	0	1	0	0
	Mode 3	0	1	0	0
Support	**100**	**G1**	**G2**	**G3**	**G4**
	Mode 1	0.1699	-0.9574	0.1699	-0.1599
	Mode 2	-0.4387	0.6497	-0.4387	0.4392
	Mode 3	-0.4802	0.5553	-0.4802	0.4801
Support	**10**	**G1**	**G2**	**G3**	**G4**
	Mode 1	-0.4777	0.5699	-0.4777	0.4676
	Mode 2	-0.4945	0.5157	-0.4945	0.4949
	Mode 3	-0.4981	0.5056	-0.4981	0.4981
Support	**0.0001**	**G1**	**G2**	**G3**	**G4**
	Mode 1	-0.5044	0.4956	-0.5044	0.4956
	Mode 2	-0.4998	0.5002	-0.4998	0.5002
	Mode 3	0.5000	-0.5000	0.5000	-0.5000

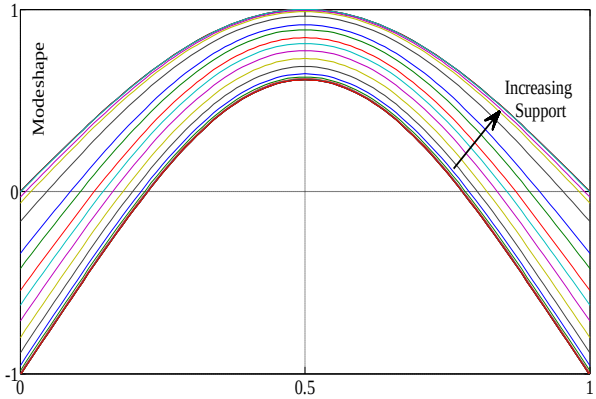

Fig.6 Fundamental modeshapes of beam vibration with elastically supported ends, with various %age end supports.

4.2 Inclusion of the rigid-body modes.

As the edge support spring constant reduces, the plate tends to a free (FFFF) plate, with zero shear force and zero bending moments at the edges. The rigid body modes of heave, pitch, and roll, become more and more prominent with decreasing 'k'. For the beam model, the heave and pitch modeshapes are respectively given as $\phi(x) = 1$; $\phi(x) = \left(1 - \frac{2x}{L}\right)$. The rigid-body modeshapes need to be included in the Eigen Value analysis. The least three frequencies obtained from it denote the heave, pitch, and roll frequencies.

Consider the extreme values of the elastic support spring constant 'k': when k→0, the rigid body modes are present; and when k→∞, they are absent. For all intermediate values of 'k', the prominence of the rigid body modes is inversely proportional to the spring constant. In this analysis, the rigid body modes are included in the free vibration analysis of beams and plates. The heave and pitch modeshapes are respectively given as $\phi(x) = 1 * \exp\left[-\frac{kL^3}{EI}\right]$; $\phi(x) = \left(1 - \frac{2x}{L}\right) * \exp\left[-\frac{kL^3}{EI}\right]$. Now

$$\exp[-k] = \frac{1}{1 + k + k^2/2! + k^3/3! + ...} = 1 - k + k^2/2! - k^3/3! + ...$$

which is bounded. The upper limit is 1 and lower limit is zero. Thus, $\exp\left[-\frac{kL^3}{EI}\right]$ serves as a suitable coefficient for the rigid body modes. The effective presence of 'k' in the denominator is justified since the heave deflection $= \frac{Force}{k}$, and the pitch angular deflection $= \frac{Moment}{kL}$.

4.3 Free Dry Vibration : elastically supported plate

With the availability of the beam modeshapes, the plate modeshape is assumed to be a weighted summation of the product of the beam modeshapes in the two directions. Galerkin's method is used to solve the Eigen value problem, generating the Eigen value (plate natural frequencies) and the Eigen vectors (weights of the Galerkin's pre-multiplier $\phi_j(x)\phi_l(y)$). The middle-term of the biharmonic operator $\nabla^4\Phi(x,y)$, in the stiffness term causes the coupling between the beam modeshapes in the two directions.

It is only for the SSSS plate, that this biharmonic operator middle-term does not couple the beam modeshapes on either side, since the beam modeshapes and their curvatures are orthogonal top each other, and drop out in the normal mode summation procedure.

Table shows the first 3x3 = 9 natural frequencies of elastically supported square plates, for four different end support factors. The unique frequencies are in **bold**, while the repeated frequencies are in *italics*. For support factor > 10^6, the plate frequencies correspond to those of a SSSS plate, which has unique and repeated frequencies. For a support factor < 10^{-3}, the plate frequencies correspond to those of a FFFF plate, which has unique, repeated, and non-repeated pairs of frequencies.

Tables 4, 5, 6 and 7 show the first 7x7 = 49 modeshapes of a square plate, with an elastic support factor of 0.0001, 10, 100, and 1000000 respectively. The diagonal modeshapes correspond to the unique frequencies for mode index = 1, 4, 9, 16, 25, 36, 49.

The first row and the first column stand for the heave interaction with all other modes. The second row and the second column stand for the pitch interaction with all other modes. Entry at position (1,1), (1,2), and (2,1) are the pure rigid body modes.

The modeshapes adjacent to the main diagonal are mirror images of each other, corresponding to the repeated frequencies modes (Identical twins). However, the alternate side-diagonal modes are very different from each other, though they have very close frequencies (Fraternal twins). Reducing the elastic support increases the prominence of the non-repeated frequency pairs.

Table 3 First 3x3=9 non-D dry natural frequencies of a square plate with four different elastic support factors.

k	1E+06	100	10	1E-04
1	**19.739**	**26.341**	**33.854**	**35.298**
2	*49.348*	*67.678*	*72.175*	*72.535*
3	*49.348*	*67.678*	*72.175*	*72.535*
4	**78.957**	**103.00**	**104.90**	**105.22**
5	*98.696*	128.86	130.07	129.66
6	*98.696*	128.87	133.53	133.74
7	*128.30*	*160.11*	*160.57*	*160.67*
8	*128.30*	*160.11*	*160.57*	*160.67*
9	**177.65**	**211.78**	**211.35**	**211.32**

Table 4 First 7x7=49 modeshapes of a square plate with elastic support factor = 1/10000.

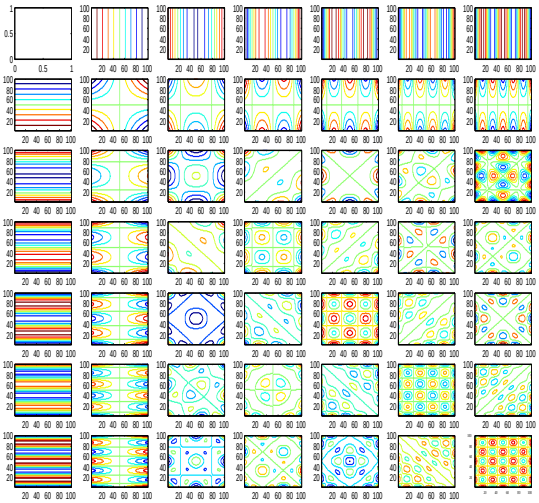

Table 5 First 7x7=49 modeshapes of a square plate with elastic support factor = 10.

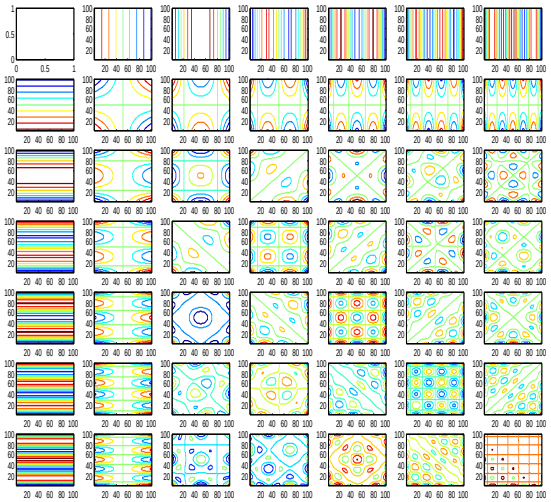

Table 6 First 7x7=49 modeshapes of a square plate with elastic support factor = 100.

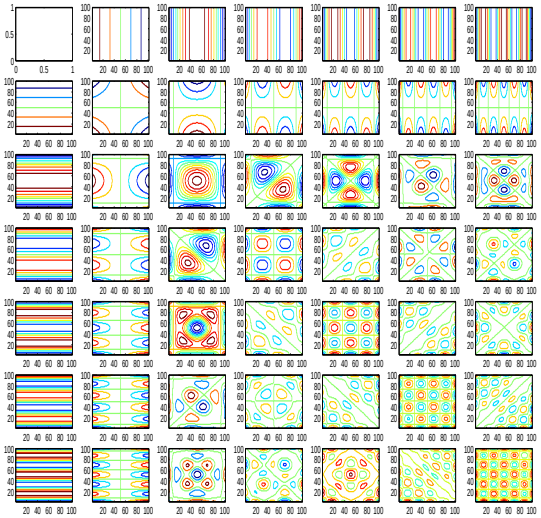

Table 7 First 7x7=49 modeshapes of a square plate with elastic support factor = 1000000.

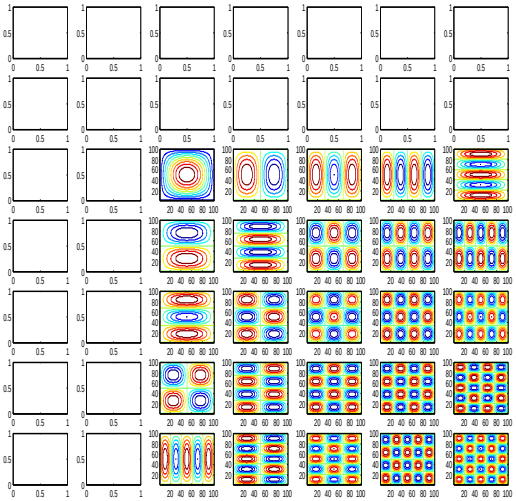

4.4 Free Wet Vibration : elastically supported plate

Inclusion of the fluid inertia reduces the natural frequencies (Table 8), making it more susceptible to transient impact loads. It is seen that the diagonal term A_{kk} is (much) larger than the non-diagonal terms A_{kn}. Since the mass matrix is diagonal and the added mass matrix shown is almost diagonal, the k^{th} wet natural frequency is given as

$$\omega_{k,wet} \equiv \omega_{k,dry} \sqrt{\frac{1}{1+A_{kk}/M_{kk}}};$$

$$M_{kk} = \int_0^L \int_0^B \Phi_k m \Phi_k \, dxdy, \quad A_{kk} = \int_0^L \int_0^B \Phi_k \rho_{water} \Psi^* \, dxdy,$$

which gives the ratio of the fluid kinetic energy to the solid kinetic energy (Table 9). The k^{th} added mass depends on the volume enclosed under the k^{th} plate modeshape.

Table 8 First 3x3 = 9 non-D wet natural frequencies of a square plates with four different elastic support factors.

k	1E+06	100	10	1E-04
1	7.8282	12.039	24.480	26.017
2	26.829	45.074	54.289	55.030
3	26.829	45.074	54.289	55.030
4	47.795	76.596	81.142	81.671
5	59.688	93.722	102.50	102.85
6	62.070	93.962	102.63	103.16
7	84.358	124.61	127.28	127.56
8	84.358	124.61	127.28	127.56
9	122.98	169.88	170.52	170.58

Table 9 NAVMI factors of the first 3x3 = 9 modeshapes of square plates with four different elastic support factors.

k	1E+06	100	10	1E-04
1	0.4104	0.2902	0.0696	0.0642
2	0.1825	0.0961	0.0576	0.0551
3	0.1825	0.0961	0.0576	0.0551
4	0.1324	0.0619	0.0514	0.0505
5	0.1328	0.0683	0.0477	0.0462
6	0.1170	0.0675	0.0481	0.0464
7	0.1006	0.0498	0.0455	0.0452
8	0.1006	0.0498	0.0455	0.0452
9	0.0832	0.0424	0.0425	0.0427

5. Forced Vibration

With the availability of the free vibration (natural) frequencies and modeshapes, the analysis proceeds to the forced vibration of the elastically supported floating plate, subject to the moving point load. The normal mode summation method fails to decouple flexural degrees of freedom (except of SSSS plate), causing the necessity of matrix inversion in the time integration of the coupled system of modal governing differential equations.

Fig.7 shows the transient aircraft load, as a function of time, modeled as a point load moving across the plate in the X-direction, with the Y-coordinate constant. The displacement has a parabolic relation with the taxiing time, as can be seen from the top view of the above diagram, with the locus of the aircraft following the black dotted line. The initial velocity of the craft is assumed to be 60 m/sec, the taxiing distance is 90% of the length

L, and the final velocity is zero, and hence the deceleration is computed as 2.25 m/s^2.

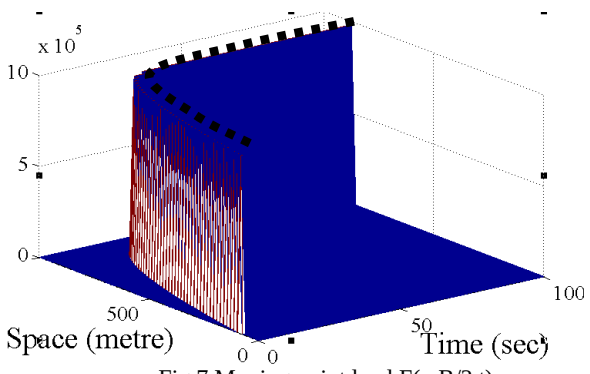

Fig.7 Moving point load F(x,B/2,t)

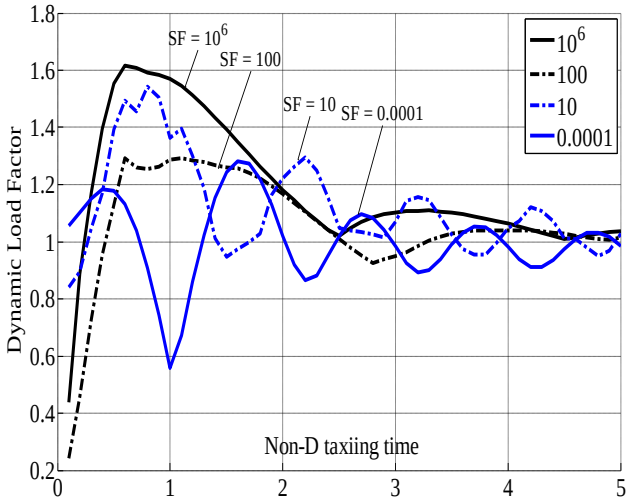

Fig. 8 DLF vs. Non-D taxiing time for square plates with four different support factors.

Fig. 8 shows the Dynamic Loading factor (DLF) for a square plate, elastically supported with support factors of 1000000 (SSSS plate), 100, 10, and 1/10000 (FFFF plate). At larger taxiing time (Non-D taxiing time > 5), the maximum dynamic deflection is only 5%-10% greater than the maximum static deflection. Since small flexural amplitudes are assumed in the Kirchhoff's plate vibration, the stresses are linearly proportional to the deflection. Thus, the dynamic stresses developed due to the decelerating aircraft load, is 5%-10% greater than that predicted through the static analysis. However, at shorter taxiing time, the dynamic stress overshoots to 30%-60% above the static stress. At very small taxiing time, to load moves across so fast that the structure does not get the time to respond, while the static analysis over-predicts the deflection due to a moving impulse function (Dirac Delta function across space).

Since the change in the behavior from free-free to simply-supported is seen between support factors of 10 and 100, the nature of the DLF also changes between these two magnitudes of the support. The DLF of the SSSS plate, subject to impact loads, may be verified from Datta (2010). As seen in Fig.8, the DLF for support factor = 1000000 (SSSS) and 100 have similar characteristics. The peak DLF decreases with decreasing elastic edge supports of the plate.

Between support factor of 100 and 10, the plate behavior switches from a nearly SSSS plate to a nearly FFFF plate. In this zone, the DLF characteristics show more frequent oscillations over the same taxing time range, as seen for DLF of plates with support factor 10 and 0.0001. This is due to the larger prominence of the rigid body modes in the normal mode summation of the force vibration GDE. Rigid body motions (heave, pitch, roll) offset the flexural deflections under the same moving load, reducing the dynamic stresses. However, too little elastic support increases the rigid body motions, which adversely affect the performance of the floating airport, and leads to radiation waves which erode the nearby shore and disturb the naval traffic in its vicinity. An optimized choice of the elastic support is necessary to avoid this. When the added mass is included in the forced vibration GDE, and the taxiing time is non-dimensionlized by the first wet flexural period of the plate, the wet DLF characteristics replicate the dry DLF (Datta 2010).

6. Discussion

A modal analysis of elastically supported square floating plates is presented. The dry vibration analysis has been done by the Galerkin's method, including the rigid body modeshapes. Wet vibration analysis has been done using the flexural modeshapes, to establish the wet natural frequencies. The various degenerate modeshapes with unique frequencies, identical twins, and fraternal twins have been established for different elastic supports. Wet vibration analysis, with water on one side of the plate, is used to generate the modal added masses.

This is followed by the forced vibration analysis of a square plate, with water on one side. Dynamic loading factors of the flexural deflection are calculated for a range of taxiing time. Optimum support factor ranges are recommended, which causes lower dynamic stresses, without exciting too much of the rigid body degrees-of-freedom.

Nomenclature

L	Length of the plate
B	Width of the plate
h	Thickness of the plate
ρ	Density of the beam material
ρ_{water}	Density of water
E	Elastic modulus of the material
I	Second moment of area of the cross-section of the beam about the horizontal neutral axis
x	space variable along x-direction
y	space variable along y-direction
t	time variable
$\phi_j(x)$	j^{th} beam modeshape in the x-direction
$\phi_l(y)$	l^{th} beam modeshape in the y-direction
$\Phi_k(x,y)$	k^{th} Plate modeshape
$q_j(t)$	Principal coordinate
$\Psi(x,y,z,t)$	Velocity potential of the fluid
ψ_k	k^{th} velocity potential of the fluid
ψ_k^*	k^{th} velocity potential of the fluid per unit velocity of the k^{th} principal coordinate.
A_{kn}	k^{th} generalized added mass under the n^{th} plate modeshapes.
F(x,y,t)	Transient load
ω_{n1}	Fundamental natural frequency of the plate
T_{n1}	Fundamental natural period of the plate
z(x,y,t)	Dynamic flexural deflection of the plate
$z_{st}(x,y,t)$	Static flexural deflection of the plate

References

[1] Young, D., *Vibration of Rectangular plates by the Ritz method*, Annual conference of the Applied Mechanics Division, Purdue University, Lafayette, Indiana, June 22-24, 1950.

[2] Saha, K.N., Misra, D., Pohit, G., and Ghosal, S., *Large Amplitude free vibration study of square plates under different boundary conditions through a static analysis*, Journal of Vibration and Control, 10: 1009-1028, 2004.

[3] Wang, G., Wereley, N.M., and Chang, D.C., *Analysis of Bending Vibration of rectangular plates using two-dimensional plate modes*, Journal of Aircraft, Vol.42, No.2, March-April 2005.

[4] Yeh, Y.L., Jang, M.J., and Wang, C.C., *Analyzing the free vibrations of a plate using finite difference and differential transformation method*, Applied mathematics and computation, 178(2006)493-501.

[5] Yu, S.N., Xiang, Y. and Wei, G.W., *Matched interface and boundary (MIB) method for the vibration analysis of plates*, Communications in Numerical Methods in Engineering (2008), DOI: 10.1002/cnm.1130.

[6] Chen, C.P., Huang, C.H. and Chen, Y.Y., *Vibration analysis and measurement for piezoceramic rectangular plates in resonance*, Journal of Sound and Vibration (2009), doi:10.1016/j.jsv.2009.04.025.

[7] Meyerhoff, W.K., *Added masses of thin rectangular plates calculated from potential theory*, Journal of Ship Research, 1970.

[8] Joseph, P., Muthuveerappan, G., and Ganeshan, N., *Vibrations of generally orthotropic plates in fluids*, Composite Structures 15 (1990) 25-42.

[9] Kwak, M.K., *Hydroelastic vibration of rectangular plates*, Transactions of the ASME, Vol.63, pp. 110-115, 1996.

[10] Cheung,Y.K. and Zhou, D., *Coupled Vibratory characteristics of a rectangular container bottom plate*, Journal of Fluids and Structures (2000) 14, 339-357.

[11] Robinson, N.J., and Palmer, S.C., "*A modal analysis of a rectangular plate floating on an incompressible fluid*", Journal of sound and Vibration, 142(3), 453-460, 1990.

[12] Kagemoto, H., Fujino, M., and Murai, M., "*Theoretical and experimental predictions of the hydroelastic response of a very large floating structure in waves*", Applied Ocean Research, 20, 135-144, 1998.

[13] Endo, H., *The behavior of a VLFS and an airplane during takeoff/landing run in wave condition*", Marine structure 13, 477-491, 2000.

[14] Seto, H., et al, "*Integrated hydrodynamic-structural analysis of VLFS*", Marine Structures, 18, 181-200, 2005.

[15] Hashemi, S.H., et al, "*Vibration analysis of rectangular Mindlin's plates on elastic foundations and vertically in contact with stationary fluid by the Ritz method*", Ocean Engineering, 37, 174-185, 2010.

[16] Datta, N., "*Hydroelastic response of marine structures to impact-induced vibrations*", Dissertation for Doctor of Philosophy, Naval Architecture and Marine Engineering, University of Michigan, Ann Arbor, USA. (2010)